

RESEARCH ARTICLE

YELLOW FEVER

Genomic and epidemiological monitoring of yellow fever virus transmission potential

N. R. Faria^{1*†}, M. U. G. Kraemer^{1,2,3*}, S. C. Hill^{1*}, J. Goes de Jesus^{4*}, R. S. Aguiar^{5*}, F. C. M. Iani^{6,7*}, J. Xavier⁴, J. Quick⁸, L. du Plessis¹, S. Dellicour⁹, J. Théze¹, R. D. O. Carvalho⁷, G. Baele⁹, C.-H. Wu¹⁰, P. P. Silveira⁵, M. B. Arruda⁵, M. A. Pereira⁶, G. C. Pereira⁶, J. Lourenço¹, U. Obolski¹, L. Abade^{1,11}, T. I. Vasylyeva¹, M. Giovanetti^{4,7}, D. Yi¹², D. J. Weiss¹³, G. R. W. Wint¹, F. M. Shearer¹³, S. Funk¹⁴, B. Nikolay^{15,16}, V. Fonseca^{7,17}, T. E. R. Adelino⁶, M. A. A. Oliveira⁶, M. V. F. Silva⁶, L. Sacchetto⁷, P. O. Figueiredo⁷, I. M. Rezende⁷, E. M. Mello⁷, R. F. C. Said¹⁸, D. A. Santos¹⁸, M. L. Ferraz¹⁸, M. G. Brito¹⁸, L. F. Santana¹⁸, M. T. Menezes⁵, R. M. Brindeiro⁵, A. Tanuri⁵, F. C. P. dos Santos¹⁹, M. S. Cunha¹⁹, J. S. Nogueira¹⁹, I. M. Rocco¹⁹, A. C. da Costa²⁰, S. C. V. Komninakis^{21,22}, V. Azevedo⁷, A. O. Chieppe²³, E. S. M. Araujo⁴, M. C. L. Mendonça⁴, C. C. dos Santos⁴, C. D. dos Santos⁴, A. M. Mares-Guia⁴, R. M. R. Nogueira⁴, P. C. Sequeira⁴, R. G. Abreu²⁴, M. H. O. Garcia²⁴, A. L. Abreu²⁵, O. Okumoto²⁵, E. G. Kroon⁷, C. F. C. de Albuquerque²⁶, K. Lewandowski²⁷, S. T. Pullan²⁷, M. Carroll²⁸, T. de Oliveira^{4,17,29}, E. C. Sabino²⁰, R. P. Souza¹⁹, M. A. Suchard^{30,31}, P. Lemey⁹, G. S. Trindade⁷, B. P. Drumond⁷, A. M. B. Filippis⁴, N. J. Loman⁸, S. Cauchemez^{15,16*}, L. C. J. Alcantara^{4,7*†}, O. G. Pybus^{1*†}

The yellow fever virus (YFV) epidemic in Brazil is the largest in decades. The recent discovery of YFV in Brazilian *Aedes* species mosquitoes highlights a need to monitor the risk of reestablishment of urban YFV transmission in the Americas. We use a suite of epidemiological, spatial, and genomic approaches to characterize YFV transmission. We show that the age and sex distribution of human cases is characteristic of sylvatic transmission. Analysis of YFV cases combined with genomes generated locally reveals an early phase of sylvatic YFV transmission and spatial expansion toward previously YFV-free areas, followed by a rise in viral spillover to humans in late 2016. Our results establish a framework for monitoring YFV transmission in real time that will contribute to a global strategy to eliminate future YFV epidemics.

Yellow fever (YF) is responsible for 29,000 to 60,000 deaths annually in South America and Africa (1) and is the most severe mosquito-borne infection in the tropics (2). Despite the existence of an effective YF vaccine since 1937 (3), an estimated >400 million unvaccinated people live in areas at risk of infection (4). Yellow

fever virus (YFV) is a member of the *Flaviviridae* family and is classified into four genotypes: East African, West African, South American I, and South American II (5–9). In the Americas, YFV transmission occurs mainly via the sylvatic cycle, in which nonhuman primates (NHPs) are infected by tree-dwelling mosquito vectors such

as *Haemagogus* spp. and *Sabethes* spp. (10, 11). YFV transmission can also occur via an urban cycle, in which humans are infected by *Aedes* spp. mosquitoes that feed mostly on humans (12, 13).

Brazil has recently experienced its largest-recorded YF outbreak in decades, with 2043 confirmed cases and 676 deaths since December 2016 (supplementary text and fig. S1) (14). The last YF cases in Brazil attributed to an urban cycle were in Sena Madureira, in the northern state of Acre, in 1942 (15). An intensive eradication campaign eliminated *Aedes aegypti* and YF from Brazil in the 1950s (16), but the vector became reestablished in the 1970s and *Aedes* spp. mosquitoes are now abundant across most of Brazil (17). The consequences of a reignition of urban cycle transmission in Brazil would be serious, as an estimated 35 million people in areas at risk for YFV transmission in Brazil remain unvaccinated (4). New surveillance and analytical approaches are therefore needed to monitor this risk in real time.

Yellow fever virus outbreak in Brazil, 2016–2017

Between December 2016 and the end of June 2017, there were 777 polymerase chain reaction (PCR)-confirmed human cases of YF across 10 Brazilian states—mostly in Minas Gerais (MG) (60% of cases), followed by Espírito Santo (32%), Rio de Janeiro (3%), and São Paulo (3%) (18). The fatality ratio of severe YF cases was estimated at 33.6%, comparable to previous outbreaks (19, 20). Despite the exceptional magnitude and rapid expansion of the outbreak, little is known about its genomic epidemiology. Further, it is uncertain how the virus is spreading through space, as well as between humans and NHPs, and analytical insights into the contribution of the urban cycle to ongoing transmission are lacking.

To characterize the 2017 YFV outbreak in Brazil, we first compared time series of confirmed cases in humans ($n = 683$) and NHPs ($n = 313$) reported until October 2017 by public health institutes in MG, the epicenter of the outbreak (Fig. 1, A and B, and fig. S2). The time series are strongly associated (cross-correlation coefficient = 0.97; $P < 0.001$). Both peak in late January 2017, and we estimate that human cases lag behind those in NHPs by 4 days (table S1). NHP cases are geographically more dispersed

¹Department of Zoology, University of Oxford, Oxford, UK. ²Computational Epidemiology Lab, Boston Children's Hospital, Boston, MA, USA. ³Department of Pediatrics, Harvard Medical School, Boston, MA, USA. ⁴Laboratório de Flavivirus, Instituto Oswaldo Cruz, FIOCRUZ, Rio de Janeiro, Brazil. ⁵Laboratório de Virologia Molecular, Departamento de Genética, Instituto de Biologia, Universidade Federal do Rio de Janeiro, Rio de Janeiro, Brazil. ⁶Laboratório Central de Saúde Pública, Instituto Octávio Magalhães, FUNED, Belo Horizonte, Minas Gerais, Brazil. ⁷Instituto de Ciências Biológicas, Universidade Federal de Minas Gerais, Belo Horizonte, Minas Gerais, Brazil. ⁸Institute of Microbiology and Infection, University of Birmingham, Birmingham, UK. ⁹Department of Microbiology and Immunology, Rega Institute, KU Leuven, Leuven, Belgium. ¹⁰Department of Statistics, University of Oxford, Oxford, UK. ¹¹The Global Health Network, University of Oxford, Oxford, UK. ¹²Department of Statistics, Harvard University, Cambridge, MA, USA. ¹³Malaria Atlas Project, Big Data Institute, Nuffield Department of Medicine, University of Oxford, Oxford, UK. ¹⁴Faculty of Epidemiology and Population Health, London School of Hygiene and Tropical Medicine, London, UK. ¹⁵Mathematical Modelling of Infectious Diseases and Center of Bioinformatics, Institut Pasteur, Paris, France. ¹⁶CNRS UMR2000: Génomique Évolutive, Modélisation et Santé, Institut Pasteur, Paris, France. ¹⁷KwaZulu-Natal Research, Innovation and Sequencing Platform (KRISP), School of Laboratory Medicine and Medical Sciences, University of KwaZulu-Natal, Durban, South Africa. ¹⁸Secretaria de Estado de Saúde de Minas Gerais, Belo Horizonte, Minas Gerais, Brazil. ¹⁹Núcleo de Doenças de Transmissão Vetorial, Instituto Adolfo Lutz, São Paulo, Brazil. ²⁰Instituto de Medicina Tropical e Faculdade de Medicina da Universidade de São Paulo, São Paulo, Brazil. ²¹Retrovirology Laboratory, Federal University of São Paulo, São Paulo, Brazil. ²²School of Medicine of ABC (FMABC), Clinical Immunology Laboratory, Santo André, São Paulo, Brazil. ²³Coordenação de Vigilância Epidemiológica do Estado do Rio de Janeiro, Rio de Janeiro, Brazil. ²⁴Departamento de Vigilância das Doenças Transmissíveis da Secretaria de Vigilância em Saúde, Ministério da Saúde, Brasília-DF, Brazil. ²⁵Secretaria de Vigilância em Saúde, Coordenação Geral de Laboratórios de Saúde Pública, Ministério da Saúde, Brasília-DF, Brazil. ²⁶Organização Pan-Americana da Saúde/Organização Mundial da Saúde - (OPAS/OMS), Brasília-DF, Brazil. ²⁷Public Health England, National Infections Service, Porton Down, Salisbury, UK. ²⁸NIHR HPRU in Emerging and Zoonotic Infections, Public Health England, London, UK. ²⁹Centre for the AIDS Programme of Research in South Africa (CAPRISA), Durban, South Africa. ³⁰Department of Biostatistics, UCLA Fielding School of Public Health, University of California, Los Angeles, CA, USA. ³¹Department of Biomathematics and Human Genetics, David Geffen School of Medicine at UCLA, University of California, Los Angeles, CA, USA.

*These authors contributed equally to this work.

†Corresponding author. Email: nuno.faria@zoo.ox.ac.uk (N.R.F.); luiz.alcantara@ioc.fiocruz.br (L.C.J.A.); oliver.pybus@zoo.ox.ac.uk (O.G.P.)

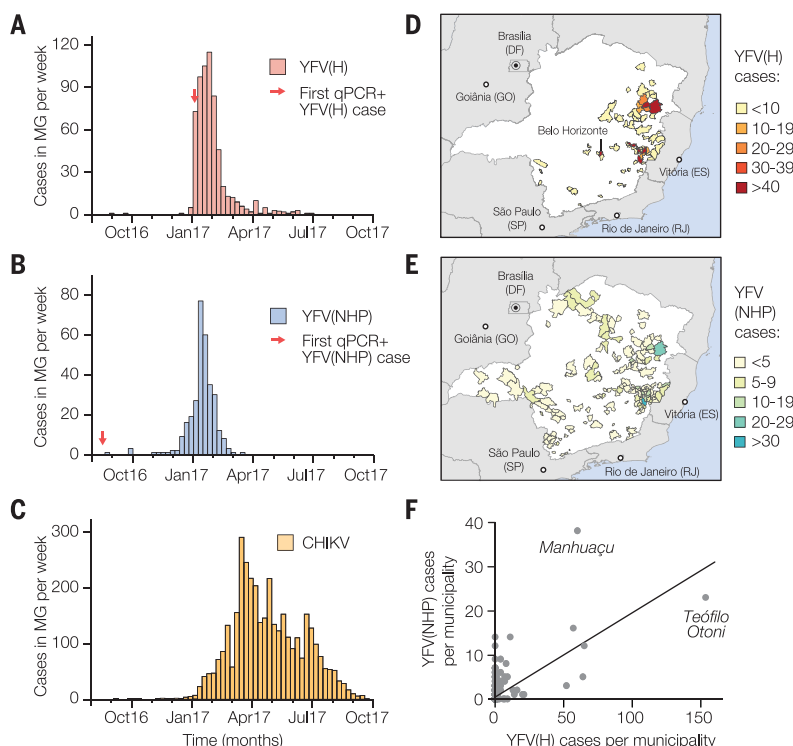


Fig. 1. Spatial and temporal epidemiology of YFV and CHIKV in Minas Gerais (MG).

(A) Time series of human (H) YFV cases in MG (676 cases across 61 municipalities)—confirmed by serology, reverse transcription quantitative PCR (RT-qPCR), or virus isolation—during the first YFV epidemic wave (August 2016 to October 2017). (B) Same as in (A) but showing NHP YFV cases (313 cases across 90 municipalities) confirmed by RT-qPCR. (C) Same as in (A) but showing human CHIKV cases (3668 cases across 129 municipalities). (D) Geographic distribution of human YFV cases in MG. (E) Geographic distribution of NHP YFV cases in MG. Figure S3 shows the corresponding geographic distribution of CHIKV cases. (F) Association between the number of human and NHP cases in each municipality of MG (Pearson's $r = 0.62$; $P < 0.0001$; nonparametric Spearman's rank $\rho = 0.32$; $P < 0.05$).

in MG than human cases, which are more concentrated in the Teófilo Otoni and Manhuaçu municipalities (Fig. 1, D and E). Despite this, the numbers of human and NHP cases per municipality are positively correlated (Fig. 1F).

To establish whether human cases are acquired in proximity to potential sources of sylvatic infection, we estimated the distance between the municipality of residence of each human case and the nearest habitat of potential transmission, determined by using the enhanced vegetation index (EVI) (21) (supplementary materials). The average minimum distance between areas with $EVI > 0.4$ and the residence of confirmed human cases is only 5.3 km. In contrast, a randomly chosen resident of MG lives, on average, ≥ 51 km away from areas with $EVI > 0.4$. Similarly, human YFV cases reside, on average, 1.7 km from the nearest NHP case, whereas the mean minimum distance of a randomly chosen MG resident to the nearest NHP case is 39.1 km. This is consistent with YF infection risk being greatest for people who reside or work in forested areas where sylvatic transmission occurs. We find that most human cases (98.5%) were reported in municipalities with estimated YFV vaccination coverage above the 80% threshold recommended by the World Health Organization (WHO). On average, human cases would need to travel 65 km from their place of residence to reach an area where vaccination coverage is $< 80\%$ (4).

Risk of YFV urban transmission

YFV was detected in *Aedes albopictus* mosquitoes caught in MG in January 2017 (22). Further, experiments suggest that *Aedes* spp. mosqui-

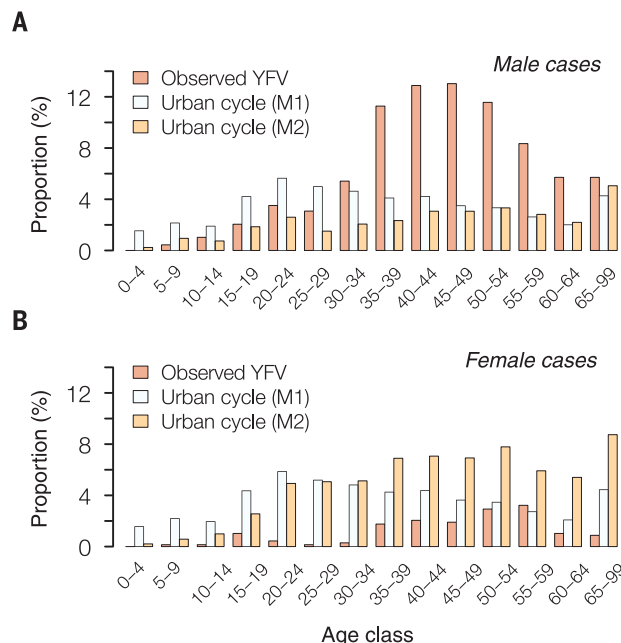


Fig. 2. Age and sex distribution of YFV cases in MG, 2016–2017.

Red bars show the proportion of observed YFV cases in MG that occur in each age class, in (A) males and (B) females. These empirical distributions are different from those predicted under two models (M1, pale blue bars; M2, orange bars) of urban cycle transmission (see text for details).

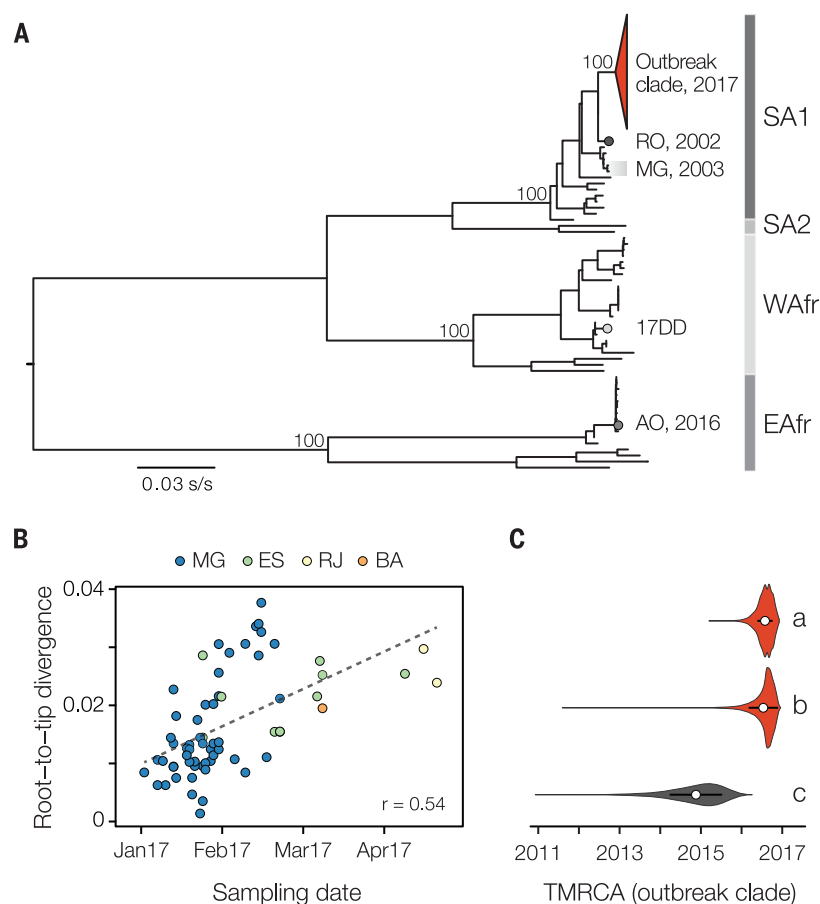
toes from southeast Brazil can transmit Brazilian YFV, although perhaps less effectively than vectors from elsewhere in the country (23, 24). It is therefore important to investigate whether YFV cases in MG occur where and when *Aedes* spp. vectors are active. To do so, we analyzed confirmed chikungunya virus (CHIKV) cases from MG (Fig. 1C).

CHIKV is transmitted by the urban mosquitoes *Ae. aegypti* and *Ae. albopictus* (25). There

were 3755 confirmed CHIKV cases in MG during January 2015 to October 2017. The CHIKV epidemic in MG in 2017 began later and lasted longer than the YFV outbreak (Fig. 1C), consistent with the hypothesis that YFV and CHIKV in the region are transmitted by different vector species. However, 29 municipalities with human YFV cases also reported CHIKV cases (Fig. 1D and fig. S3), indicating that YFV is indeed present in municipalities with *Aedes* mosquitoes. The mean

Fig. 3. Molecular phylogenetics of the Brazilian YFV epidemic.

(A) Maximum likelihood phylogeny of complete YFV genomes showing the outbreak clade (red triangle) within the South American I (SA1) genotype (Fig. 4 and fig. S6). SA2, WAfr, and EAfr indicate the South America II, West Africa, and East Africa genotypes, respectively. For clarity, five YFV strains introduced to Venezuela from Brazil (49) are not shown. The scale bar is in units of substitutions per site (s/s). Node labels indicate bootstrap support values. RO 2002, strain BeH655417 from Roraima; MG 2003, two strains from the previous YF outbreak in MG in 2003; 17DD, the vaccine strain used in Brazil; AO 2016, YFV outbreak Angola in 2015–2016 (13). **(B)** Root-to-tip regression of sequence sampling date against genetic divergence from the root of the outbreak clade (fig. S6). Sequences are colored according to sampling location (MG, Minas Gerais; ES, Espírito Santo; RJ, Rio de Janeiro; BA, Bahia). **(C)** Violin plots showing estimated posterior distributions (white circles denote means) of the time of the most recent common ancestor (TMRCA) of the outbreak clade. Estimates were obtained using two different datasets (gray, SA1 genotype; red, outbreak clade) and under different evolutionary models: a, uncorrelated lognormal relaxed clock (UCLN) model with a skygrid tree prior with covariates specifically, the time series data shown in Fig. 1, A to C; also see fig. S7); b, UCLN model with a skygrid tree prior without covariates; c, fixed local clock model (see supplementary materials).



YFV vaccination rate in districts with both YFV and CHIKV cases is 72.6% (range = 61 to 78%) (4). Thus, relatively high vaccination rates in the locations in MG where YF spillover to humans occurs, and potentially lower vector competence (23, 24), may ameliorate the risk of establishment of an urban YFV cycle in the state. However, adjacent urban regions (including São Paulo and Rio de Janeiro) have lower vaccination rates (4), receive tens of millions of visitors per year (26), and have recently experienced many human YFV cases (20). Thus, the possibility of sustained urban YFV transmission in southern Brazil and beyond necessitates continual virological and epidemiological monitoring.

We sought to establish a framework to evaluate routes of YFV transmission during an outbreak from the characteristics of infected individuals. Specifically, we assessed whether an outbreak is driven by sylvatic or urban transmission by comparing the age and sex distributions of observed YFV cases with those expected under an urban cycle in MG. For example, an individual's risk of acquiring YFV via the sylvatic cycle depends on their likelihood to travel to forested areas, an occurrence that is typically highest among male adults (27). In contrast, under an urban cycle, we expect more uniform exposure across age and sex classes, similar to that observed for urban cases in Paraguay (28) and Nigeria (29).

The male-to-female sex ratio of reported YFV cases in MG is 5.7 (85% of cases are male), and incidence is highest among males aged 40 to 49 (Fig. 2). We compared this distribution to that expected under two models of urban cycle transmission (supplementary materials). In model M1, age and sex classes vary in vaccination status but are equally exposed to YFV, a scenario that is typical of arboviral transmission (30). Under model M1, predicted cases are characterized by a sex ratio ~1, and incidence peaks among individuals aged 20 to 25 (Fig. 2). In model M2, we assume that the pattern of YFV exposure among age and sex classes follows that observed for CHIKV. The sex ratio of reported CHIKV cases in MG is 0.49 (33% of cases are male) (fig. S4). Under model M2, predicted incidence is highest in females aged >30. The discrepancy between the observed distribution and that predicted under the two urban cycle models indicates that the YF epidemic in MG is dominated by sylvatic transmission. This method shows that age- and sex-structured epidemiological data can be used to qualitatively evaluate the mode of YFV transmission during an outbreak.

Genomic surveillance of the Brazilian YFV outbreak

During a YF outbreak, it is important to undertake virological surveillance to (i) track epidemic origins and transmission hotspots, (ii) character-

ize genetic diversity to aid molecular diagnostics, (iii) detect viral mutations associated with disease severity, and (iv) exclude the possibility that human cases are caused by vaccine reversion. We generated 62 complete YF genomes from infected humans ($n = 33$) and NHPs ($n = 29$) from the most affected Brazilian states, including MG ($n = 51$), Espírito Santo ($n = 8$), Rio de Janeiro ($n = 2$), and Bahia ($n = 1$) (Fig. 3 and table S3). We also report two genomes from samples collected in 2003 during a previous YFV outbreak in MG from 2002 to 2003 (31). Genomes were generated in Brazil using a combination of methods (tables S5 to S7); half were generated in MG using a MinION portable YFV sequencing protocol adapted from (32) (tables S4 and S5). This protocol was made publicly available in May 2017 after the completion of pilot sequencing experiments using a cultured vaccine strain (supplementary materials). Median genome coverages were similar for samples obtained from NHPs [99%; median cycle threshold value (Ct) = 11] and from human cases (99%; median Ct = 16) (tables S5 to S7).

To put the newly sequenced YFV genomes in a global context, we added our genomes to a pool of 61 publicly available genomes (33, 34). We developed and applied an automated online phylogenetic tool to identify and classify YFV gene sequences (also publicly available, see supplementary materials). Phylogenies estimated by

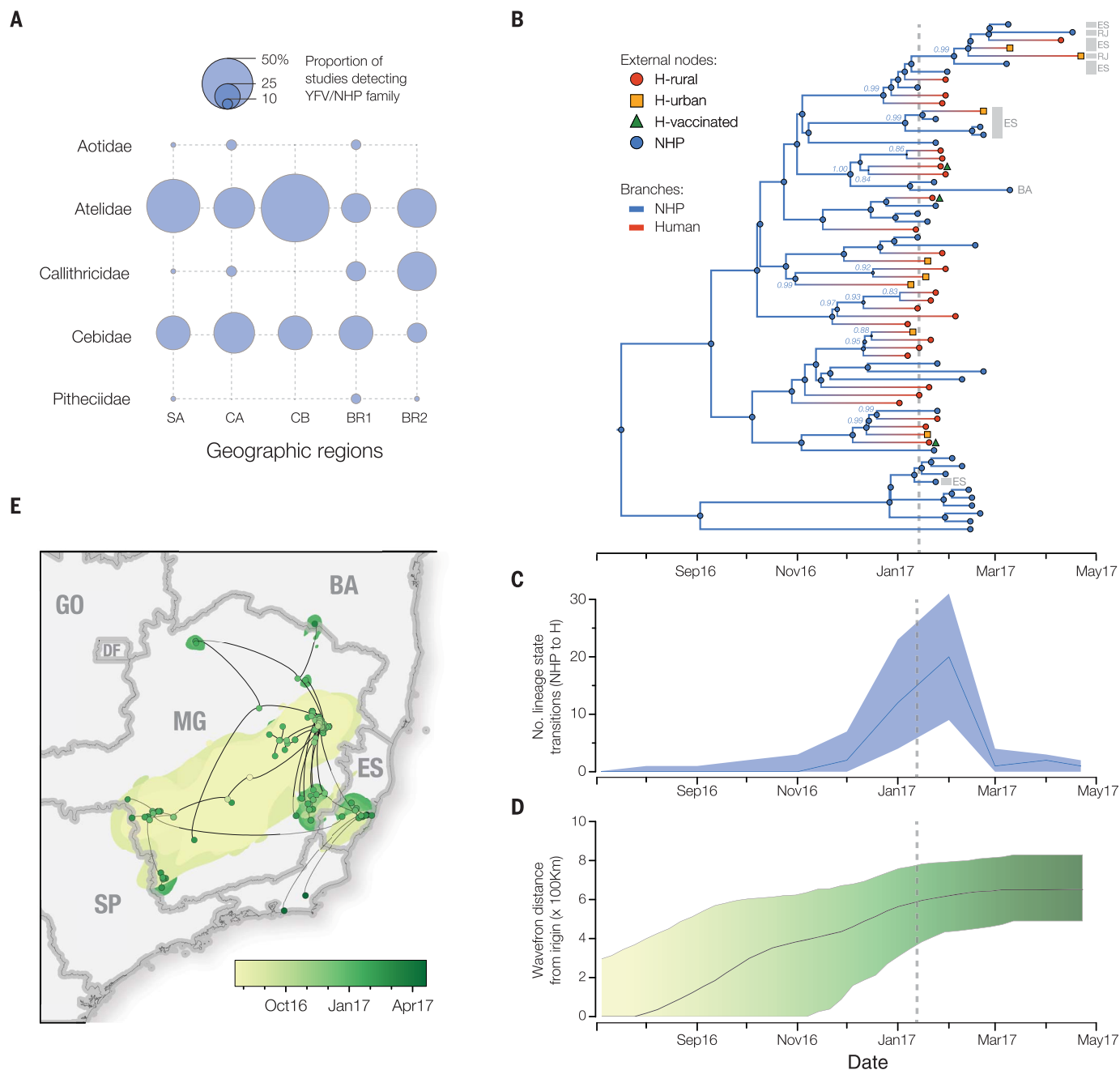


Fig. 4. Spatial and evolutionary dynamics of YFV outbreak. (A) Frequency of detection of YFV in NHPs in the Americas (50). Circle sizes represent the proportion of published studies ($n = 15$) that have detected YFV in each primate family and region. SA, South America (except Brazil); CA, Central America; CB, Caribbean; BR1, Brazil (before 2017); BR2, Brazil (this study). (B) Maximum clade credibility phylogeny inferred under a two-state (human and NHP) structured coalescent model. External node symbols denote sample type. Gray bars and labels indicate sample location (RJ, Rio de Janeiro; ES, Espírito Santo; BA, Bahia; others were sampled in MG). Internal nodes whose posterior state probabilities are >0.8 are annotated by circles. Node labels indicate posterior state probabilities for selected nodes. Internal branches are blue for NHPs and red for humans. Figure S8 shows a fully annotated tree. (C) Average number of YFV phylogenetic state

transitions (from NHPs to humans) per month. Solid line, median estimate; shaded area, 95% BCI. **(D)** Expansion of the YFV epidemic wavefront estimated using a continuous phylogeographic approach (35). At each time point the plot shows the maximum spatial distance between phylogeny branches and the inferred location of outbreak origin. Solid line, median estimate; shaded area, 95% BCI. The dashed lines in (B) to (D) indicate when YF was declared a public health emergency in MG (13 January 2017). **(E)** Reconstructed spatiotemporal diffusion of the YFV outbreak. Phylogeny branches are arranged in space according to the locations of phylogeny nodes (circles). Locations of external nodes are known, whereas those of internal nodes are inferred (44). DF, Distrito Federal; GO, Goiás; SP, São Paulo. Shaded regions represent 95% credible regions of internal nodes. Nodes and uncertainty regions are colored according to time.

this tool, along with maximum likelihood and Bayesian methods, consistently place the Brazilian outbreak strains in a single clade within the South America I (SAI) genotype with maximum statistical support (bootstrap = 100%; posterior probability > 0.99) (Fig. 3A and fig. S5).

The outgroup to the outbreak clade is strain BeH655417, a human case sampled in Alto Alegre, Roraima, north Brazil, in 2002. In contrast, isolates sampled during the previous outbreak in MG in 2003 are more distantly related to the outbreak clade within the SAI genotype (Fig. 3A). Thus, the 2017 outbreak was more likely caused by a YFV strain introduced from an endemic area, possibly northern or center-west Brazil (35), than by the reemergence of a lineage that had persisted in MG. Although low sampling densities mean that this conclusion is provisional, similar scenarios have been suggested for previous Brazilian epizootics (36). The 14-year gap between the current outbreak and the date of the most closely related nonoutbreak strain agrees with the reported periodicity of YF outbreaks in northern Brazil (37), thought to be dictated by vector abundance and the accumulation of susceptible NHP hosts (19, 38).

At least seven humans from MG with PCR-confirmed YFV received a YF vaccine before the onset of symptoms. To test that these occurrences were caused by natural infection, and not by vaccine reactivation, we sequenced the YFV genomes from three of these cases (Fig. 3A and table S3). Our phylogenetic analysis clearly shows that these represent natural infections caused by the ongoing outbreak and are conclusively not derived from the 17DD vaccine strain (which belongs to the West African YFV genotype) (Fig. 3A and fig. S6).

Unifying YFV epidemiology and molecular evolution

Virus genomes are a valuable source of information about epidemic dynamics (39) but are rarely used to investigate specific YFV outbreaks in detail. Here we show how a suite of three analytical approaches, which combine genetic, epidemiological, and spatial data, can provide insights into YFV transmission.

First, we used a Bayesian method (40) to explore potential covariates of fluctuations in the effective population size of the YFV outbreak in 2017. After finding that genetic divergence in the outbreak clade accumulates over the time scale of sampling (Fig. 3B and fig. S6), albeit weakly, we sought to determine which epidemiological time series best describe trends in inferred YFV effective population size. We found that effective population size fluctuations of the YFV outbreak are well explained by the dynamics of both human and NHP YFV cases (inclusion probability: 0.37 for human cases and 0.63 for NHP cases) (table S8). These two YFV time series explain the genetic diversity dynamics of the ongoing outbreak 10^3 times more effectively than CHIKV incidence (inclusion probability <0.001), which represents transmission by *Aedes* spp. vectors. One benefit of this approach is that epidemiological

data contribute to estimation of the outbreak time scale. By incorporating YFV incidence data into evolutionary inference, we estimate the time of the most recent common ancestor (TMRCA) of the outbreak clade to be late July 2016 [95% Bayesian credible interval (BCI): March to November 2016] (Fig. 3C and fig. S7), consistent with the date of the first PCR-confirmed case of YFV in a NHP in MG (Jul 2016). The uncertainty around the TMRCA estimate is reduced by 30% when epidemiological and genomic data are combined, compared with genetic data alone (Fig. 3C).

Second, to better understand YFV transmission between humans and NHPs, we measured the movement of YFV lineages between the NHP reservoir and humans, using a phylogenetic structured coalescent model (41). Although previous studies have confirmed that YFV is circulating in five neotropical NHP families (Aotidae, Atelidae, Callitrichidae, Pitheciidae, and Cebidae) (Fig. 4A), thus far NHP YFV genomes during the 2017 outbreak have been recovered only from *Alouatta* spp. (family Cebidae) (33). In this analysis, we used the TMRCA estimate obtained above (Fig. 3C) to inform the phylogenetic time scale (Fig. 4B). All internal nodes in the outbreak phylogeny whose host state is well supported (posterior probability >0.8) are inferred to belong to the NHP population, consistent with an absence of urban transmission and in agreement with the large number of NHP cases reported in southeast Brazil (20). Despite this, we caution that hypotheses of human-to-human transmission linkage should not be tested directly using phylogenetic data alone, owing to the large undersampling of NHP infections. Notably, the structured coalescent approach reveals substantial changes in the frequency of NHP-to-human host transitions through time, rising from zero around November 2016 and peaking in February 2017 (Fig. 4C). This phylogenetic trend matches the time series of confirmed YFV cases in MG (Fig. 1, A and B), demonstrating that viral genomes, when analyzed using appropriate models, can be used to quantitatively track the dynamics of zoonosis during the course of an outbreak (42).

Third, we used a phylogenetic relaxed random walk approach to measure the outbreak's spatial spread (43) (supplementary materials and methods and table S9). When projected through space and time (Fig. 4, D and E, and movie S1), the phylogeny shows a southerly dissemination of virus lineages from their inferred origin in MG toward densely populated areas, including Rio de Janeiro and São Paulo (where YF vaccination was not recommended until July 2017 and January 2018, respectively). We estimate that virus lineages move, on average, 4.25 km/day (95% BCI: 2.64 to 10.76 km/day) (44). This velocity is similar when human YFV terminal branches are removed (5.3 km/day) and therefore most likely reflects YFV lineage movement within the sylvatic cycle and not the movement of asymptomatic infected humans. These rates are higher than expected given the distances

typically travelled by NHPs in the region (45) and suggest the possibility that YFV lineage movement may have been aided by human activity—e.g., transport of infected mosquitoes in vehicles (46) or hunting or illegal trade of NHPs in the Atlantic forest (47, 48). The epidemic wavefront (maximum distance of phylogeny branches from the inferred epidemic origin) expanded steadily between August 2016 and February 2017 at an estimated rate of ~3.3 km/day. Therefore, by the time YF was declared a public health emergency in MG (13 January 2017; dashed lines in Fig. 4, B to D), the epidemic had already expanded ~600 km (Fig. 4D) and caused >100 reported cases in both humans and NHPs (Fig. 1). Notably, the first detection in humans in December 2016 was concomitant with the outbreak's spatial expansion phase (Fig. 4D) and the rise in estimated NHP-to-human zoonoses (Fig. 4C); both were likely driven by an increase in the abundance of sylvatic vectors. Thus, the outbreak lineage appeared to circulate among NHPs in a widening geographic area for several months before human cases were detected.

Conclusion

Epidemiological and genomic surveillance of human and animal populations at risk is crucial for early detection and rapid containment of YFV transmission. The YFV epidemic in Brazil continues to unfold with an increase in cases since December 2017. Longitudinal studies of NHPs are needed to understand how YFV lineages disseminate across South America between outbreaks and how epizootics are determined by the dynamics of susceptible animals in the reservoir. To achieve the WHO's goal to eliminate YF epidemics by 2026, YF surveillance necessitates a global, coordinated strategy. Our results and analyses show that rapid genomic surveillance of YFV, when integrated with epidemiological and spatial data, could help anticipate the risk of human YFV exposure through space and time and monitor the likelihood of sylvatic versus urban transmission. We hope that the toolkit introduced here will prove useful in guiding YF control in a resource-efficient manner.

REFERENCES AND NOTES

1. T. Garske et al., *PLOS Med.* **11**, e1001638 (2014).
2. C. I. Paules, A. S. Fauci, *N. Engl. J. Med.* **376**, 1397–1399 (2017).
3. M. Theiler, H. H. Smith, *J. Exp. Med.* **65**, 767–786 (1937).
4. F. M. Shearer et al., *Lancet Infect. Dis.* **17**, 1209–1217 (2017).
5. M. R. Nunes et al., *J. Virol.* **86**, 13263–13271 (2012).
6. J. P. Mutebi, H. Wang, L. Li, J. E. Bryant, A. D. T. Barrett, *J. Virol.* **75**, 6999–7008 (2001).
7. J. J. von Lindern et al., *J. Gen. Virol.* **87**, 895–907 (2006).
8. E. Wang et al., *Virology* **225**, 274–281 (1996).
9. G. J. Chang, B. C. Cropp, R. M. Kinney, D. W. Trent, D. J. Gubler, *J. Virol.* **69**, 5773–5780 (1995).
10. M. N. O. Segura, F. C. C. Castro, *Atlas de Culicídeos na Amazônia Brasileira* (Instituto Evandro Chagas Press, 2007), vol. 167.
11. J. da C. Cardoso et al., *Emerg. Infect. Dis.* **16**, 1918–1924 (2010).
12. A. A. Grobbelaar et al., *Emerg. Infect. Dis.* **22**, 1854–1855 (2016).
13. M. U. G. Kraemer et al., *Lancet Infect. Dis.* **17**, 330–338 (2017).
14. O. Franco, *História da Febre-Amarela no Brasil* (Ministério da Saúde, DNERU, 1969).

15. R. A. G. B. Consoli, R. Lourenço de Oliveira, *Principais Mosquitos de Importância Sanitária no Brasil* (FioCruz, 1994).
16. J. Vainio, "Yellow fever" (World Health Organization, 1998).
17. M. U. Kraemer *et al.*, *eLife* **4**, e08347 (2015).
18. Secretaria de Vigilância em Saúde, Ministério da Saúde, "Emergência epidemiológica de febre amarela no Brasil, no período de Dezembro de 2016 a Julho de 2017" (Boletim Epidemiológico vol. 48, 2017); http://portalarquivos2.saude.gov.br/images/pdf/2017/setembro/06/2017_027.pdf.
19. P. F. Vasconcelos *et al.*, *J. Med. Virol.* **65**, 598–604 (2001).
20. Pan American Health Organization/World Health Organization, "Epidemiological update yellow fever 16 Feb 2018" (PAHO/WHO, 2018); www.paho.org/hq/index.php?option=com_topics&view=read&id=2194&Itemid=40784&lang=en.
21. F. M. Shearer *et al.*, *Lancet Glob. Health* **6**, e270–e278 (2018).
22. Instituto Evandro Chagas, www.iec.gov.br/portal/descoberta/ (2018).
23. R. Lourenço-de-Oliveira, M. Vazeille, A. M. B. de Filippis, A. B. Failloux, *Trans. R. Soc. Trop. Med. Hyg.* **98**, 43–54 (2004).
24. D. Couto-Lima *et al.*, *Sci. Rep.* **7**, 4848 (2017).
25. N. R. Faria *et al.*, *PLOS Currents Outbreaks*, 10.1371/currents.outbreaks.c97507e3e48efb946401755d468c28b2 (2016).
26. N. R. Faria *et al.*, *Sci. Rep.* **7**, 15216 (2017).
27. S. H. Tuboi, Z. G. A. Costa, P. F. da Costa Vasconcelos, D. Hatch, *Trans. R. Soc. Trop. Med. Hyg.* **101**, 169–175 (2007).
28. PAHO, "Outbreak of Yellow Fever in Paraguay" (PAHO, 2009).
29. A. Nasidi *et al.*, *Trans. R. Soc. Trop. Med. Hyg.* **83**, 401–406 (1989).
30. S. D. Thiberville *et al.*, *PLOS Negl. Trop. Dis.* **7**, e2004 (2013).
31. M. Ribeiro, C. M. F. Antunes, *Rev. Soc. Bras. Med. Trop.* **42**, 523–531 (2009).
32. J. Quick *et al.*, *Nat. Protoc.* **12**, 1261–1276 (2017).
33. M. C. Bonaldo *et al.*, *Mem. Inst. Oswaldo Cruz* **112**, 447–451 (2017).
34. A. Moreira-Soto *et al.*, *Clin. Microbiol. Infect.* 10.1016/j.cmi.2018.01.026 (2018).
35. Secretaria de Vigilância em Saúde, Ministério da Saúde, "Reemergência da Febre Amarela Silvestre no Brasil, 2014/2015: Situação epidemiológica e a importância da vacinação preventiva e da vigilância intensificada no período sazonal" (Boletim Epidemiológico vol. 46, 2015); <http://portalarquivos2.saude.gov.br/images/pdf/2015/outubro/19/2015-032-FA-ok.pdf>.
36. P. F. C. Vasconcelos *et al.*, *Emerg. Infect. Dis.* **10**, 1578–1584 (2004).
37. F. P. Câmara, A. L. B. B. Gomes, L. M. F. Carvalho, L. G. V. Castello, *Rev. Soc. Bras. Med. Trop.* **44**, 297–299 (2011).
38. P. F. Vasconcelos *et al.*, *Cad. Saude Publica* **17** (suppl.), 155–164 (2001).
39. G. Dudas *et al.*, *Nature* **544**, 309–315 (2017).
40. M. S. Gill, P. Lemey, S. N. Bennett, R. Biek, M. A. Suchard, *Syst. Biol.* **65**, 1041–1056 (2016).
41. T. G. Vaughan, D. Kühnert, A. Poppinga, D. Welch, A. J. Drummond, *Bioinformatics* **30**, 2272–2279 (2014).
42. G. Dudas, L. M. Carvalho, A. Rambaut, T. Bedford, *eLife* **7**, e31257 (2018).
43. O. G. Pybus *et al.*, *Proc. Natl. Acad. Sci. U.S.A.* **109**, 15066–15071 (2012).
44. P. Lemey, A. Rambaut, J. J. Welch, M. A. Suchard, *Mol. Biol. Evol.* **27**, 1877–1885 (2010).
45. L. Jung, I. Mourthe, C. E. V. Grelle, K. B. Strier, J. P. Boubli, *PLOS ONE* **10**, e0129789 (2015).
46. E. Flacio, L. Engeler, M. Tonolla, P. Müller, *Parasit. Vectors* **9**, 304 (2016).
47. A. Estrada *et al.*, *Sci. Adv.* **3**, e1600946 (2017).
48. R. A. Nascimento, R. A. M. Montano, *Neotrop. Biol. Conserv.* **8**, 79–87 (2013).
49. A. J. Auguste *et al.*, *Emerg. Infect. Dis.* **21**, 99–102 (2015).
50. P. R. Stephens *et al.*, *Ecology* **98**, 1476 (2017).

ACKNOWLEDGMENTS

We thank FUNED-MG and the Brazilian YFV surveillance network for their contributions. N.R.F. thanks J. F. Drexler for sharing data. N. Trovão for discussions. F. Campos for proof imaging, and P. Fonseca for proofreading. We thank Oxford Nanopore Technologies for technical support. L.C.J.A. thanks QIAGEN for reagents and equipment. A.C.d.C. and E.C.S. thank Illumina, Zymo Research, Sage Science, and Promega for donation of reagents. **Funding:** This work was supported in part by CNPq 400354/2016-0 and FAPESP 2016/01735-2. N.R.F. is supported by a Sir Henry Dale Fellowship (204311/Z/16/Z), internal GCRF grant 005073, and John Fell Research Fund grant 005166. This research received funding from the ERC (grant agreement 614725-PATHPHYLODYN) and from the Oxford Martin School. M.U.G.K. acknowledges funding from a Branco Weiss Fellowship, administered by ETH Zurich, a Training Grant from the National Institute of Child Health and Human Development (T32HD040128), and the National Library of Medicine of the National Institutes of Health (R01LM010812 and R01LM011965). S.D. is funded by the Fonds Wetenschappelijk Onderzoek (FWO, Flanders, Belgium). G.B. acknowledges support from the Interne Fondsen KU Leuven/Internal Funds KU Leuven. A.C.d.C. is funded by FAPESP 2017/00021-9.

B.B.N. and S.C. are supported by the EU's Horizon 2020 Programme through ZIKAlliance (grant 734548), the Investissement d'Avenir program, the Laboratoire d'Excellence Integrative Biology of Emerging Infectious Diseases program (grant ANR-10-LABX-62-IBED), the Models of Infectious Disease Agent Study of the National Institute of General Medical Sciences, the AXA Research Fund, and the Association Robert Debré. P.L. and M.A.S. acknowledge funding from the European Research Council (grant agreement 725422-ReservoirDOCS) and from the Wellcome Trust Collaborative Award 206298/Z/17/Z. P.L. acknowledges support from the Research Foundation, Flanders (Fonds voor Wetenschappelijk Onderzoek, Vlaanderen, G066215N, G0D5117N, and G0B9317N).

Author contributions: N.R.F., L.C.J.A., S.C.H., A.M.B.F., M.U.G.K., S.C., and O.G.P. designed the study. S.C.H., J.J.G., R.S.d.A., F.C.M.J., J.X., R.D.O.C., J.T., M.G., L.C.J.A., and N.R.F. undertook fieldwork. S.C.H., J.Q., J.J.G., A.C.d.C., S.C.V.K., V.F., and T.d.O. undertook experiments. N.R.F., L.d.P., J.T., S.D., G.B., O.G.P., C.-H.W., T.I.V., and P.L. performed genetic analyses. M.U.G.K., S.C., S.F., J.L., U.O., L.A., D.Y., and N.R.F. performed epidemiological and cartographic analyses. B.N., F.M.S., and N.R.F. performed historical YFV review. N.R.F., M.U.G.K., L.C.J.A., S.C., and O.G.P. wrote the manuscript. E.C.S., J.T., L.d.P., R.P.S., P.L., C.F.C.d.A., R.S.d.A., and A.M.B.F. edited the manuscript. All other authors were involved in collection, processing, sequencing, and bioinformatics of samples and geographic data. All authors read and approved the contents of the manuscript. **Competing interests:** N.J.L. and L.C.J.A. received free-of-charge reagents in support of the project from Oxford Nanopore Technologies. A.C.d.C. and E.C.S. received reagents at no cost from Illumina, Zymo Research, Sage Science, and Promega. **Data and materials availability:** Raw data, code, and analysis files are available via the GitHub repository (<https://github.com/arbospread/YFV-monitoring>). See <https://github.com/zibraject/zika-pipeline/tree/master/schemes> for MinION sequencing protocols. Genome sequences generated here are available under GenBank accession numbers MH018064 to MH018115 and MH484423 to MH484434.

SUPPLEMENTARY MATERIALS

www.sciencemag.org/content/361/6405/894/suppl/DC1
Materials and Methods
Supplementary Text
Figs. S1 to S10
Tables S1 to S9
References (51–107)
Movie S1

31 March 2018; accepted 20 July 2018
Published online 23 August 2018
10.1126/science.aat7115

Genomic and epidemiological monitoring of yellow fever virus transmission potential

N. R. FariaM. U. G. KraemerS. C. HillJ. Goes de JesusR. S. AguiarF. C. M. IaniJ. XavierJ. QuickL. du PlessisS. DellicourJ. ThézéR. D. O. CarvalhoG. BaeleC.-H. WuP. P. SilveiraM. B. ArrudaM. A. PereiraG. C. PereiraJ. LourençoU. ObolskiL. AbadeT. I. VasylyevaM. GiovanettiD. YiD. J. WeissG. R. W. WintF. M. ShearerS. FunkB. NikolayV. FonsecaT. E. R. AdelinoM. A. A. OliveiraM. V. F. SilvaL. SacchettoP. O. Figueiredol. M. RezendeE. M. MelloR. F. C. SaidD. A. SantosM. L. FerrazM. G. BritoL. F. SantanaM. T. MenezesR. M. BrindeiroA. TanuriF. C. P. dos SantosM. S. CunhaJ. S. Nogueiral. M. RoccoA. C. da CostaS. C. V. KomninakisV. AzevedoA. O. ChieppeE. S. M. AraujoM. C. L. MendonçaC. C. dos SantosC. D. dos SantosA. M. Mares-GuiaR. M. R. NogueiraP. C. SequeiraR. G. AbreuM. H. O. GarciaA. L. AbreuO. OkumotoE. G. KroonC. F. C. de AlbuquerqueK. LewandowskiS. T. PullanM. CarrollT. de OliveiraE. C. SabinoR. P. SouzaM. A. SuchardP. LemeyG. S. TrindadeB. P. DrumondA. M. B. FilippisN. J. LomanS. CauchemezL. C. J. AlcantaraO. G. Pybus

Science, 361 (6405),

Arbovirus risk in Brazil

Despite the existence of an effective vaccine for yellow fever, there are still almost 80,000 fatalities from this infection each year. Since 2016, there has been a resurgence of cases in Africa and South America—and this at a time when the vaccine is in short supply. The worry is that yellow fever will spread from the forests to the cities, because its vector, *Aedes* spp. mosquitoes, are globally ubiquitous. Faria *et al.* integrate genomic, epidemiological, and case distribution data from Brazil to estimate patterns of geographic spread, the risks of virus exposure, and the contributions of rural versus urban transmission (see the Perspective by Barrett). Currently, the yellow fever epidemic in Brazil seems to be driven by infections acquired while visiting forested areas and indicates spillover from susceptible wild primates.

Science, this issue p. 894; see also p. 847

View the article online

<https://www.science.org/doi/10.1126/science.aat7115>

Permissions

<https://www.science.org/help/reprints-and-permissions>

Use of think article is subject to the [Terms of service](#)